Testing Inner CGM Virialization: Connecting CGM Emission to Central Galaxy Evolution with FIRE-2

Braedyn Kim[1,2], Elizabeth Mone[2], Kung-Yi Su[2], Claude-André Faucher-Giguère[2]

1. Department of Physics, University of Illinois at Urbana-Champaign, 1110 W Green St Loomis Laboratory, Urbana, IL 61801
2. Center for Interdisciplinary Exploration and Research in Astrophysics (CIERA), Northwestern University, 1800 Sherman Ave, Evanston, IL 60201

bkim235@illinois.edu

Background

- The circumgalactic medium (CGM): the envelope around a galaxy and extending to its virial radius
  - Plays a significant role in galaxy formation and evolution
- Haloes virialize from the outside in -> a process known as inner CGM virialization (ICV) (Stern et al. 2021).
  - The **pre-ICV state is connected to bursty dwarfs** and the **post-ICV state is connected to steady, thin disk galaxies.**
- CGM emission mapping is a potentially powerful way to test these predictions.
- Emission in the CGM has historically been difficult to observe because the gas is very faint.
  - The Modular Optical Telephoto Hyperspectral Robotic Array (MOTHRA) telescope (Lokhorst 2019) will map out the CGM that could not previously be detected.
  - We use FIRE-2 simulations to create **Hα and [OIII] emission maps** and corresponding surface brightness profiles of the CGM before and after ICV.

Comparing predicted CGM surface brightness maps and profiles with MOTHRA observations allows the connection between inner CGM virialization and the evolution of central galaxy properties to be tested

Simulations

- The FIRE-2 simulations used in this work vary in the mass of the central halo and how it evolves over time. We selected two galaxy suites for this analysis, including **five dwarf galaxies with $M_{Halo}{\sim}10^{11}M_{\odot}$** and **three Milky-Way mass galaxies with $M_{Halo}{\sim}10^{12}M_{\odot}$.**
- We analyze the galaxies at z = 0, when the five dwarf galaxies we study are all in the pre-ICV state and the three Milky-Way mass galaxies are in the post-ICV state (Sultan et al. 2026).

Methods

- To calculate the surface brightness of Hα and [OIII] we first calculate the emissivity, which depends on the galaxy redshift, temperature, metallicity, n_H, and identified emission line.
  - **We use CLOUDY look up tables to solve for the emissivity and luminosity** (Ploeckinger & Schaye 2020).
- Surface brightness maps are generated by creating a 2d projection of the luminosity, which returns a value per area that we can use to obtain the surface brightness values for profiles and maps at various directions.
  - We choose to **default our analysis to an edge on view** to emphasize the difference in morphology between the pre-ICV and post-ICV.

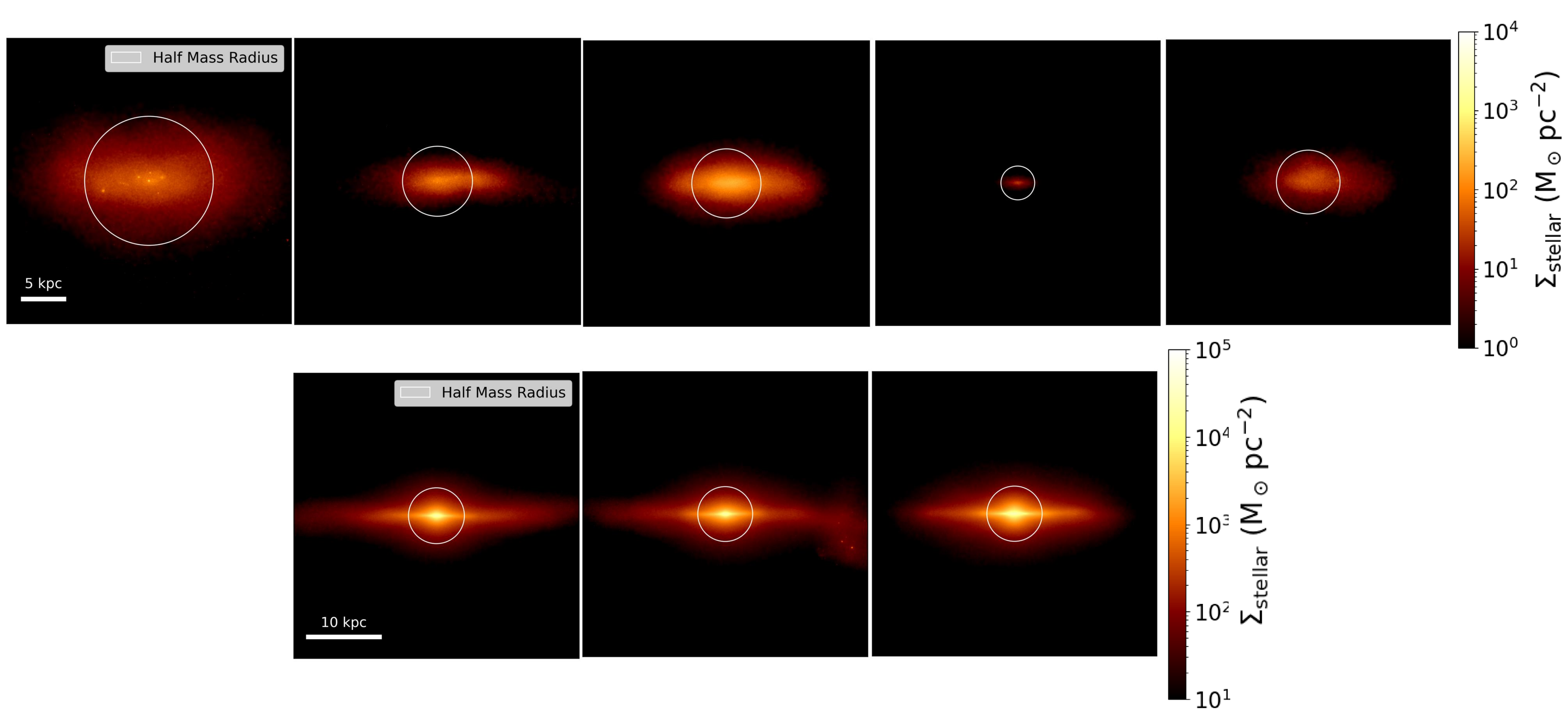

Fig. 1: Stellar images of the pre-ICV galaxies (dwarf galaxies) on the top row and post-ICV (Milky-Way mass galaxies) on the bottom row. The pre-ICV galaxies are characterized by an irregular morphology, while the post-ICV galaxies have a thin disk.

Results: Surface Brightness Profiles

- The pre-ICV and post-ICV H-alpha and [OIII] surface brightness profiles are shown in Fig. 2.
- We find that **for the pre-ICV state, there is a more gradual decline**. Meanwhile, for the post-ICV state there is a more sudden drop or "cliff" where the surface brightness drops. We find that the slope in the post-ICV is also steeper than the pre-ICV slopes, ~1.6x the slope for Hα and the slope for [OIII]. We also find the slope for various edge-on angles, which gives us errors for the slope.

Key Finding: Steeper Slope Found for Post-ICV Profiles

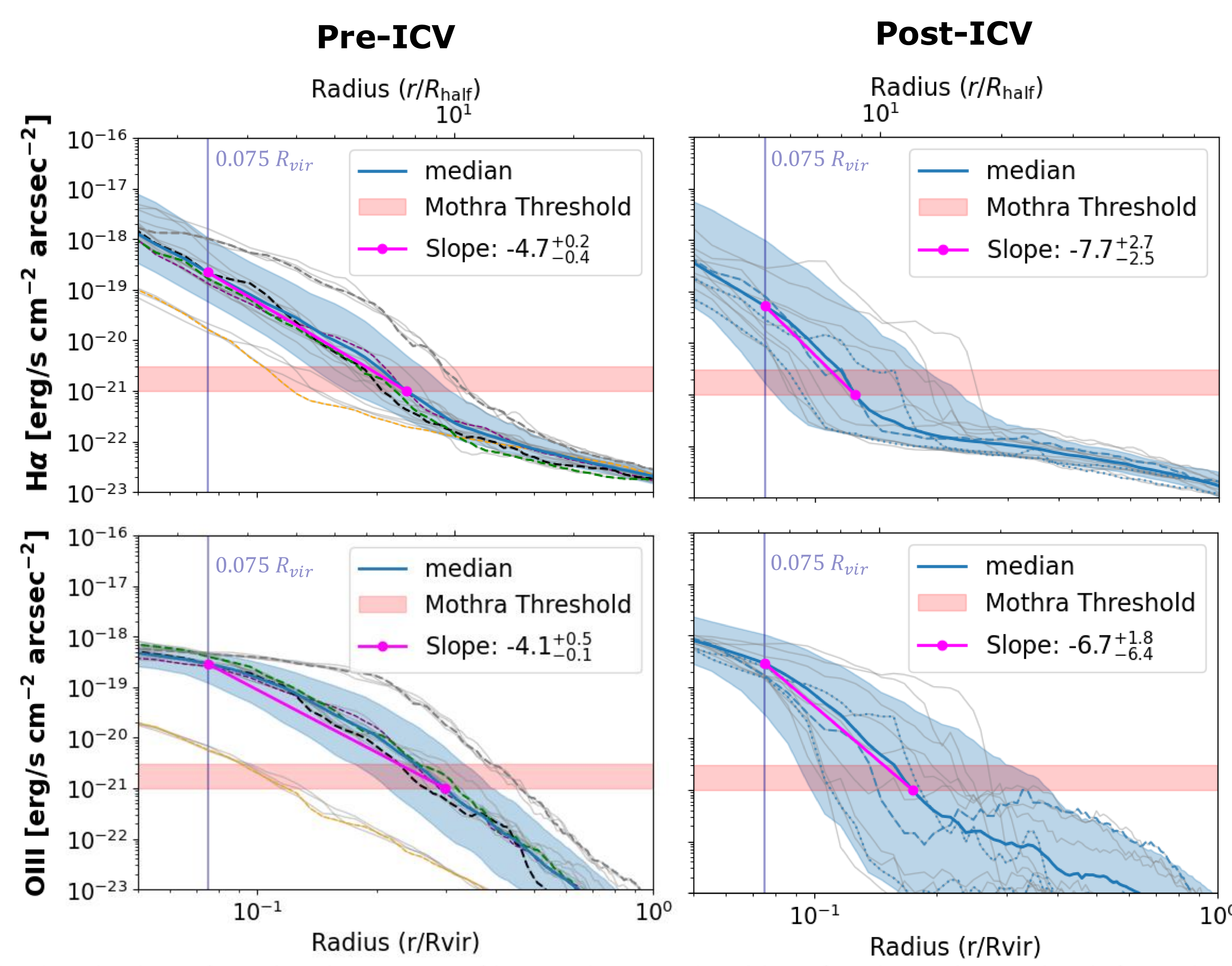

Fig 2. Stacked surface brightness profiles with pre-ICV (dwarf galaxies) on the left and post-ICV (Milky-Way mass galaxies) on the right, at z = 0. The 5 individual dwarf galaxies are plotted as dashed lines, with varying colors. The 3 individual Milky-Way mass galaxies are plotted as separate line styles. The MOTHRA threshold is plotted as a red band to represent where the surface brightness remains detectable. The slope is plotted in pink and calculated between slightly outside the center of the galaxy, 0.075 R_{vir}(virial radius), to the point where the surface brightness becomes undetectable. The gray lines are the surface brightness profiles of various edge on viewing angles.

Results: Emission Maps

- Representative Hα and [OIII] surface brightness maps are shown in Fig. 3.
- The surface brightness maps for the pre-ICV state are found to be more diffuse.
- The post-ICV state corresponds to a disk morphology as seen in the stellar images.

Pre-ICV maps are irregular and asymmetric while the post-ICV maps resemble a thin disk.

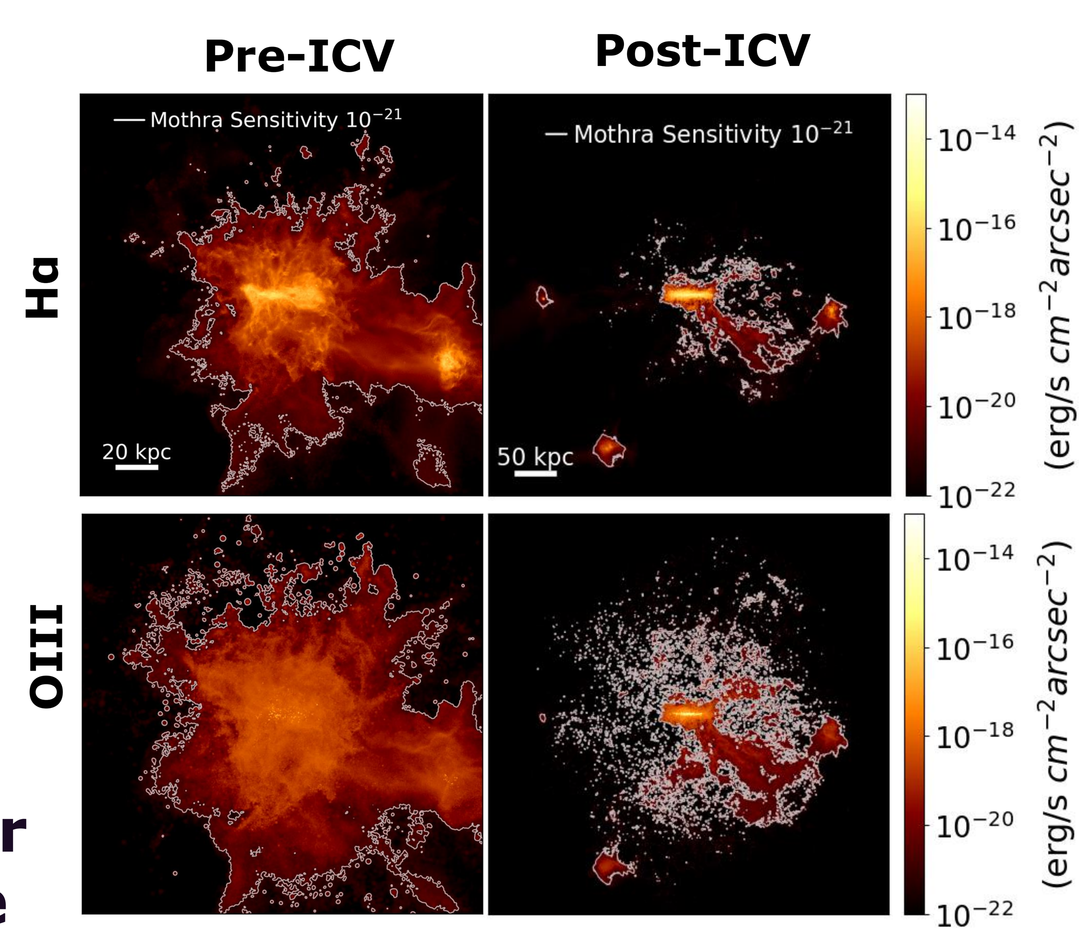

Fig 3. Surface brightness maps, with contours of the MOTHRA sensitivity threshold in white.

Conclusions and Future Work

- We find that there is a clear observational signature of the pre-ICV and post-ICV states, with a steeper slope in the post-ICV surface brightness profiles and a disk morphology in the post-ICV surface brightness maps. These differences can then be used to compare with MOTHRA observations to test predictions about the connection between inner CGM virialization and the diskiness of central galaxies.
- Future work includes **expanding the statistics to include other FIRE galaxy simulations suites**, such as $M_{Halo}{\sim}10^{10}M_{\odot}$ galaxies and more $M_{Halo}{\sim}10^{12}M_{\odot}$ galaxies. We can also **expand on the emission lines we analyze**, such as additionally looking at OVI.

Acknowledgments and References

This material is based upon work supported by the U.S. National Science Foundation (NSF) under Award Number AST-2446392, a Research Experience for Undergraduates (REU) grant awarded to CIERA at Northwestern University. Any opinions, findings, and conclusions or recommendations expressed in this material are those of the author(s) and do not necessarily reflect the views of the NSF. Additional support was provided by NSF through grants AST-2108230 and AST-2307327; by NASA through grant 80NSSC22k0809; and by BSF through grant #2024262. We also thank Imad Pasha, Chloe Neufeld, and Deborah Lokhorst for useful discussions regarding MOTHRA capabilities.

Stern, J., Faucher-Giguère, C.-A., Fielding, D., et al. 2021, ApJ, 911, 88.
Lokhorst, D., Abraham, R., van Dokkum, P., Wijers, N., & Schaye, J. 2019, ApJ, 877, 4
Sultan, I., Faucher-Giguère, C.-A., Stern, J., & Sun, G. 2026, MNRAS, 550, 1.
Ploeckinger, S., & Schaye, J. 2020, MNRAS, 497, 4857